8   Studying Continuous Symmetry Breaking with Exact Diagonalization

A.M. Läuchli, M. Schuler, and A. Wietek
Institut für Theoretische Physik
Universität Innsbruck

Contents

1 Introduction

Spontaneous symmetry breaking is amongst the most important concepts in condensed matter physics. The fact that a ground or thermal state of a system does not obey its full symmetry explains most of the well-known phase transitions in solid state physics like crystallization of a fluid, superfluidity, magnetism, superconductivity, and many more. A standard concept for investigating spontaneous symmetry breaking is the notion of an order parameter. In the thermodynamic limit it is non-zero in the symmetry-broken phase and zero in the disordered phase.

Another concept to detect spontaneous symmetry breaking less widely known but equally powerful is the *tower of states analysis* (TOS) [1, 2]. The energy spectrum, i.e., the eigenvalues of the Hamiltonian of a *finite* system in a symmetry-broken phase, has a characteristic and systematic structure: several eigenstates are quasi-degenerate on finite systems and become degenerate in the thermodynamic limit and possess certain quantum numbers. The TOS analysis deals with understanding the spectral structure and predicting quantum numbers of the groundstate manifold. Also on finite systems spontaneous symmetry breaking manifests itself in the structure of the energy spectra which are accessible via numerical simulations. Most prominently the Exact Diagonalization method [3, 4] can exactly calculate these spectra and quantum numbers on moderate system sizes. The predictions of TOS analyses are highly nontrivial statements which can be used to unambiguously identify symmetry-broken phases. Thus TOS analysis is a powerful technique to investigate many condensed matter systems using numerical simulations. The goal of these lecture notes is to explain the specific structure of energy spectra and their quantum numbers in symmetry-broken phases. The anticipated structure is then compared to several actual numerical simulations using Exact Diagonalization.

These lecture notes have been written at the kind request of the organizers of the Jülich 2016 Autumn School on Correlated Electrons. The notes build on and complement previously available lecture notes by Claire Lhuillier [2], by Grégoire Misguich and Philippe Sindzingre [5] and by Karlo Penc and one of the authors [3].

The outline of these notes is as follows: in Section 2 we introduce the tower of states of continuous symmetry breaking and derive its scaling behavior. We investigate a toy model which shows most of the relevant features. Section 3 explains in detail how the multiplicities and quantum numbers in the TOS can be predicted by simple group theoretical methods. To apply these methods we discuss several examples in Section 4 and compare them to actual numerical data from Exact Diagonalization.

2 Tower of states

We start our discussion of spontaneous symmetry breaking of continuous symmetries by investigating the Heisenberg model on the square lattice. Its Hamiltonian is given by

$$H = J \sum_{\langle i,j \rangle} \mathbf{S}_i \cdot \mathbf{S}_j \tag{1}$$

and is invariant under global $SU(2)$ spin rotations, i.e., a rotation of every spin on each site with the same rotational $SU(2)$ matrix. Therefore the total spin

$$\mathbf{S}_{\text{tot}}^2 = \left(\sum_i \mathbf{S}_i \right)^2 = S_{\text{tot}}(S_{\text{tot}} + 1) \tag{2}$$

is a conserved quantity of this model and every state in the spectrum of this Hamiltonian can be labeled via its total spin quantum number. The Heisenberg Hamiltonian on the square lattice has the property of being *bipartite*: The lattice can be divided into two sublattices A and B such that every term in Eq. (1) connects one site from sublattice A to sublattice B. It was found out early [1] that the groundstate of this model bears resemblance with the classical *Néel state*

$$|\text{Néel class.}\rangle = |\uparrow\downarrow\uparrow\downarrow \cdots\rangle \tag{3}$$

where the spin-ups live on the A sublattice and the spin-downs live on the B sublattice. This state does not have the total spin as a good quantum number. From elementary spin algebra we know that it is rather a superposition of several states with different total spin quantum numbers. For example the 2-site state

$$|\uparrow\downarrow\rangle = \frac{|\uparrow\downarrow\rangle - |\downarrow\uparrow\rangle}{2} + \frac{|\uparrow\downarrow\rangle + |\downarrow\uparrow\rangle}{2} = |S_{\text{tot}} = 0, m = 0\rangle + |S_{\text{tot}} = 1, m = 0\rangle \tag{4}$$

is the superposition of a singlet ($S_{tot} = 0$) and a triplet ($S_{tot} = 1$). Therefore if such a state were to be a groundstate of Eq. (1) several states with different total spin would have to be degenerate. It turns out that on finite bipartite lattices this is not the case: The total groundstate of the Heisenberg model on bipartite lattices can be proven to be a singlet state with $S_{\text{tot}} = 0$. This result is known as *Marshall's Theorem* [6–8]. So how can a Néel state resemble the singlet groundstate? To understand this we drastically simplify the Heisenberg model and investigate a toy model whose spectrum we can fully understand analytically.

2.1 Toy model: the Lieb-Mattis model

By introducing the Fourier-transformed spin operators

$$\mathbf{S}_{\mathbf{k}} = \frac{1}{\sqrt{N}} \sum_{j=0}^{N} e^{i\mathbf{k}\cdot\mathbf{x}_j} \mathbf{S}_j \,, \tag{5}$$

we can rewrite the original Heisenberg Hamiltonian in terms of these operators as

$$H = J \sum_{\mathbf{k}\in\text{B.Z.}} \omega_{\mathbf{k}} \, \mathbf{S}_{\mathbf{k}} \cdot \mathbf{S}_{-\mathbf{k}} \,, \tag{6}$$

where $\omega_{\mathbf{k}} = \cos(k_x) + \cos(k_y)$ and the sum over $\mathbf{k}$ runs over the momenta within the first Brillouin zone. Let $\mathbf{k}_0 = (\pi, \pi)$ be the ordering wavevector which is the dual to the translations that leave the square Néel state invariant. We now want to look at the truncated Hamiltonian

$$H_{\text{LM}} = 2J \left(\mathbf{S}_{(0,0)}^2 - \mathbf{S}_{\mathbf{k}_0} \cdot \mathbf{S}_{-\mathbf{k}_0} \right) \tag{7}$$

where we omit all Fourier components in Eq. (6) except $\mathbf{k} = (0, 0)$ and $\mathbf{k}_0$. This model is called the Lieb-Mattis model [7] and has a simple analytical solution. To see this, we notice that Eq. (7) is given by

$$H_{LM} = \frac{4J}{N} \sum_{i \in A, \, j \in B} \mathbf{S}_i \cdot \mathbf{S}_j \tag{8}$$

in real space where A and B denote the two bipartite sublattices within the square lattice and each spin is only coupled with spins in the other sublattice. The interaction strength is equal regardless of the distance between the two spins. Thus this model is not likely to be experimentally relevant. Yet it will serve as an illustrative example how breaking the spin-rotational symmetry manifests itself in the spectrum of a finite size system. We can write Eq. (8) as

$$H_{LM} = \frac{4J}{N} \left(\sum_{i,j \in A \cup B} \mathbf{S}_i \cdot \mathbf{S}_j - \sum_{i,j \in A} \mathbf{S}_i \cdot \mathbf{S}_j - \sum_{i,j \in B} \mathbf{S}_i \cdot \mathbf{S}_j \right) \tag{9}$$

$$= \frac{4J}{N} (\mathbf{S}_{\text{tot}}^2 - \mathbf{S}_A^2 - \mathbf{S}_B^2) \tag{10}$$

From this it is obvious that the Lieb-Mattis model can be considered as the coupling of two large spins S_A and S_B to a total spin S_{tot}.

We find that the operators $\mathbf{S}_{\text{tot}}^2$, S_{tot}^z, $\mathbf{S}_A^2$ and $\mathbf{S}_B^2$ commute with this Hamiltonian and therefore the sublattice spins S_A and S_B as well as the total spin S_{tot} and its z-component m_{tot} are good quantum numbers for this model. For a lattice with N sites (N even) the sublattice spins can be chosen in the range $S_{A,B} \in \{0, 1, \ldots, N/4\}$ and by coupling them

$$S_{\text{tot}} \in \{|S_A - S_B|, |S_A - S_B| + 1, \ldots, S_A + S_B\} \tag{11}$$

$$m_{\text{tot}} \in \{-S_{\text{tot}}, -S_{\text{tot}} + 1, \ldots, S_{\text{tot}}\} \tag{12}$$

can be chosen.[1] A state $|S_{\text{tot}}, m, S_A, S_B\rangle$ is thus an eigenstate of the systems with energy

$$E(S_{\text{tot}}, m, S_A, S_B) = \frac{4J}{N} \left[S_{\text{tot}}(S_{\text{tot}} + 1) - S_A(S_A + 1) - S_B(S_B + 1) \right] \tag{13}$$

independent of m, so each state is at least $(2S_{\text{tot}} + 1)$-fold degenerate.

Tower of states We first want to consider only the lowest energy states for each S_{tot} sector. These states build the famous *tower of states* and collapse in the thermodynamic limit to a highly degenerate groundstate manifold, as we will see now.

For a given total spin S_{tot} the lowest energy states are built by maximizing the last two terms in Eq. (13) with $S_A = S_B = N/4$ and

$$E_0(S_{\text{tot}}) = E(S_{\text{tot}}, m, N/4, N/4) = \frac{4J}{N} S_{\text{tot}}(S_{\text{tot}} + 1) - J\left(\frac{N}{4} + 1\right). \tag{14}$$

The groundstate of a finite system will thus be the singlet state with $S_{\text{tot}} = 0$.[2] On a finite system the groundstate is, therefore, totally symmetric under global spin rotations and does not break

---

[1]This set of states spans the full Hilbert space of the model.

[2]The groundstate of the Heisenberg model Eq. (1) on a bipartite sublattice with equal sized sublattices is also proven to be a singlet state $S_{tot} = 0$ by Marshall's Theorem [8, 6, 7].

the $SU(2)$-symmetry. In the thermodynamic limit $N \to \infty$, however, the energy of all states scales to zero and all these states constitute the groundstate manifold.

The classical Néel state with fully polarized spins on each sublattice can be built out of these states by a linear combination of all the S_{tot} levels with $m_{tot} = 0$ [2]. All other Néel states pointing in a different direction in spin-space can be equivalently built out of this groundstate manifold by considering linear combinations with other m_{tot} quantum numbers. In the thermodynamic limit, any infinitesimal small field will force the Néel state to choose a direction and the groundstate spontaneously breaks the $SU(2)$-symmetry.

The states which constitute the groundstate manifold in the thermodynamic limit can be readily identified on finite-size systems as well, where their energy is given by Eq. (14). These states are called the *tower of states* (TOS) or also *Anderson tower*, *thin spectrum*, and *quasi-degenerate joint states* [1, 9–11].

Excitations   The lowest excitations above the tower of states can be built by lowering the spin of one sublattice S_A or S_B by one, see Eq. (13). Let us set $S_A = N/4$ and $S_B = N/4 - 1$ which implies that $S_{\text{tot}} \in \{1, 2, \ldots, N/2 - 1\}$. We can directly compute the energy $E_1(S_{\text{tot}})$ of these excited states for each allowed S_{tot} and the energy gap to the tower of states is constant[3]

$$E_{\text{exc}}(S_{\text{tot}}) = E_1(S_{\text{tot}}) - E_0(S_{\text{tot}}) = J \, . \tag{15}$$

As the energy gap is constant, the lowest excitations of the Lieb-Mattis model are static spin-flips. The next lowest excitations are spin-flips on both sublattices, $S_A = S_B = N/4 - 1$ with excitation energy $E_{\text{exc}_2} = 2J$ and $S_{\text{tot}} \in \{0, 1, \ldots, N/2 - 2\}$. We see that the energy gap of no levels except for the TOS vanishes in the thermodynamic limit, so the TOS indeed solely contributes to the groundstate manifold.

Quantum Fluctuations   When we introduced the Lieb-Mattis model Eq. (7) from the Heisenberg model Eq. (6) we neglected all Fourier components except of $\mathbf{k} = (0, 0)$ and $\mathbf{k} = \mathbf{k}_0$. This was a quite crude approximation and it is not guaranteed that all results for the Lieb-Mattis model will survive for the short-range Heisenberg model. To get some first results regarding this question, we can introduce small quantum fluctuations on top of the Néel groundstate of the Lieb-Mattis model and perform a perturbative spin-wave analysis in first order.[4] This approach does not affect the scaling of the tower of states levels, but it has an important effect on the excitations. They are not static particles anymore, but are spinwaves (magnons) with a dispersion, which is linear around the ordering-wave vector $\mathbf{k} = \mathbf{k}_0$ and $\mathbf{k} = (0, 0)$. On a finite-size lattice the momentum space is discrete with a distance proportional to $1/L$ between them, where L is the linear size of the system. The energy of the lowest excitation above the

---

[3]This is an artifact of the infinite-range interaction in the Lieb-Mattis model. In the original Heisenberg model these modes become gapless magnon excitations.

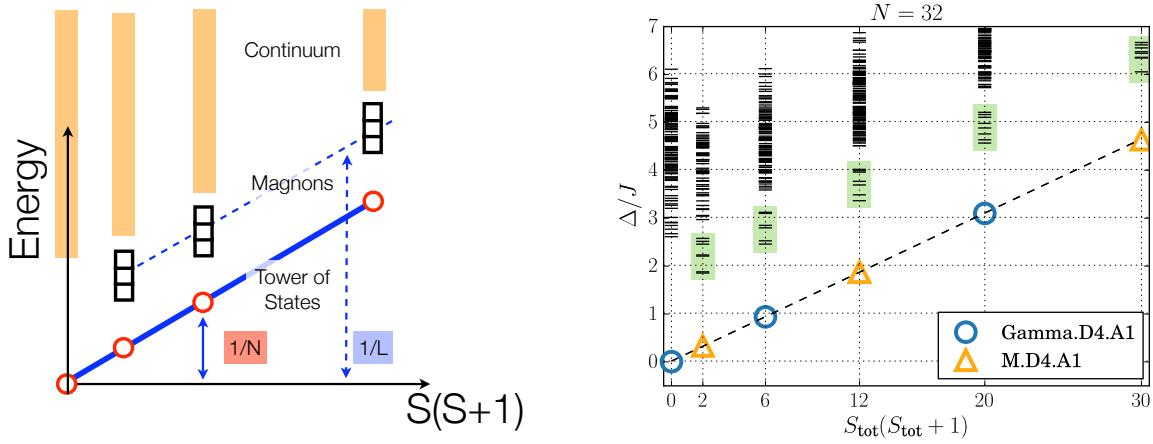[4]A more detailed discussion can be found in [2].

Fig. 1: *Left: Schematic finite-size energy spectrum of an antiferromagnet breaking $SU(2)$ spin-rotational symmetry. The TOS levels are the lowest energy levels for each total spin S and scale with $1/N$ to the groundstate energy. The low-energy magnon excitations are separated from the TOS and a continuum of higher energy states and scale with $1/L$. Right: Energy spectrum for the Heisenberg model on a square lattice. The TOS levels are connected by a dashed line. The single-magnon dispersion (green boxes) with $S_{tot} \in \{1, 2, \dots\}$ are well separated from the TOS and the higher multi-particle continuum. The different symbols represent quantum numbers related to space-group symmetries and agree with the expectations for a Néel state (See section 3).*

TOS, the single magnon gap, therefore scales as $E_{\mathrm{exc}} \propto J/L$ to zero.[5] As the scaling is, however, slower for $d > 1$-dimensional systems than the TOS scaling, these levels do not influence the groundstate manifold in the thermodynamic limit. Finally, the excitation of two magnons results in a two-particle continuum above the magnon mode.

The properties of the TOS and its excitations are summarized in Fig. 1. The left figure shows the general properties of the finite-size energy spectrum which can be expected when a continuous symmetry group is spontaneously broken in the thermodynamic limit. The right figure depicts the TOS spectrum for the Heisenberg model on a square lattice with $N = 32$ sites, obtained with Exact Diagonalization. One can clearly identify the TOS, the magnon dispersion and the many-particle continuum. The existence of a Néel TOS was not only confirmed numerically for the Heisenberg model on the square lattice, but also with analytical techniques beyond the simplification to the Lieb-Mattis model [1, 10, 11]. The different symbols in Fig. 1 represent different quantum numbers related to the space-group symmetries on the lattice. In the next section we will see that the structure of these quantum numbers depends on the exact shape of the symmetry-broken state and we will learn how to compute them.

---

[5]In the thermodynamic limit the single magnon mode is gapless and has linear dispersion around $\mathbf{k} = \mathbf{k}_0$ and $\mathbf{k} = (0, 0)$. It corresponds to the well-known Goldstone mode which is generated when a continuous symmetry is spontaneously broken.

3   Symmetry analysis

In the analysis of excitation spectra from Exact Diagonalization on finite-size simulation clusters the *tower of states analysis* (TOS) is a powerful tool to detect spontaneous symmetry breaking. Symmetry breaking implies degenerate groundstates in the thermodynamic limit. On finite-size simulation clusters this degeneracy is in general not exact. We rather expect a certain scaling of the energy differences in the thermodynamic limit. We distinguish two cases:

- **Discrete symmetry breaking:** In this case we have a degeneracy of finitely many states in the thermodynamic limit. The groundstate splitting Δ on finite size clusters scales as $\Delta \sim \exp(N/\xi)$, where N is the number of sites in the system

- **Continuous symmetry breaking:** Here the groundstate in the thermodynamic limit is infinitely degenerate. The states belonging to this degenerate manifold collapse as $\Delta \sim 1/N$ on finite size clusters as we have seen in section 2. It is important to understand that these states are not the Goldstone modes of continuous symmetry breaking. Both the degenerate groundstate and the Goldstone modes appear as low-energy levels on finite size clusters but have different scaling behaviors.

The scaling of these low-energy states can now be investigated on finite size clusters. More importantly, also the quantum numbers of these low-energy states such as momentum, pointgroup representation, or total spin can be predicted [2,5,12]. The detection of correct scaling behavior together with correctly predicted quantum numbers yields very strong evidence that the system spontaneously breaks symmetry in the way that has been anticipated. This is the TOS method. In the following we will discuss how to predict the quantum numbers for discrete as well as continuous symmetry breaking. The main mathematical tool we use is the character-formula from basic group representation theory.

Lattice Hamiltonians like a Heisenberg model often have a discrete symmetry group arising from translational invariance, pointgroup invariance, or some discrete local symmetry, like a spin-flip symmetry. In this chapter we will first discuss the representation theory and the characters of the representations of space groups on finite lattices. We will then see how this helps us to predict the representations of the degenerate ground states in discrete as well as continuous symmetry breaking.

3.1   Representation theory for space groups

For finite discrete groups such as the space group of a finite lattice the full set of irreducible representations (irreps) can be worked out. Let us first discuss some basic groups. Let's consider an $n \times n$ square lattice with periodic boundary conditions and a translationally invariant Hamiltonian like the Heisenberg model on it. In the following we will set the lattice spacing to $a = 1$. The discrete symmetry group we consider is $\mathcal{T} = \mathbb{Z}_n \times \mathbb{Z}_n$ corresponding to the group of translations on this lattice. This is an Abelian group of order n^2. Its representations can be labeled by the momentum vectors $\mathbf{k} = (\frac{2\pi i}{n}, \frac{2\pi j}{n})$, $i, j \in \{0, \cdots, n-1\}$ which just correspond

to the reciprocal Bloch vectors defined on this lattice. Put differently, the vectors $\mathbf{k}$ are the reciprocal lattice points of the lattice spanned by the simulation torus of our $n \times n$ square lattice. The character $\chi_{\mathbf{k}}$ of the $\mathbf{k}$-representation is given by

$$\chi_{\mathbf{k}}(\mathbf{t}) = \mathrm{e}^{i\mathbf{k}\cdot\mathbf{t}} \tag{16}$$

where $\mathbf{t} \in \mathcal{T}$ is the vector of translation. This is just the usual Bloch factor for translationally invariant systems.

Let us now consider a (symmorphic) space group of the form $\mathcal{D} = \mathcal{T} \times \mathrm{PG}$ as the discrete symmetry group of the lattice where PG is the pointgroup of the lattice. For a model on an $n \times n$ square lattice this could for example be the dihedral group of order 8, D_4, consisting of four-fold rotations together with reflections. The representation theory and the character tables of these point groups are well-known. Since $\mathcal{D}$ is now a product of the translation and the point group we could think that the irreducible representations of $\mathcal{D}$ are simply given by the product representations $(\mathbf{k} \otimes \rho)$ where $\mathbf{k}$ labels a momentum representation and ρ an irrep of PG. But here is a small caveat. We have to be careful since $\mathcal{D}$ is only a semidirect product of groups since translations and pointgroup symmetries do not necessarily commute. This alters the representation theory for this product of groups and the irreps of $\mathcal{D}$ are not just simply the products of irreps of $\mathcal{T}$ and PG. Instead the full set of irreps for this group is given by $(\mathbf{k} \otimes \rho_{\mathbf{k}})$ where $\rho_{\mathbf{k}}$ is an irrep of the so called *little group* $L_{\mathbf{k}}$ of $\mathbf{k}$ defined as

$$L_{\mathbf{k}} = \{g \in \mathrm{PG};\ g(\mathbf{k}) = \mathbf{k}\} \tag{17}$$

which is just the stabilizer of $\mathbf{k}$ in PG. For example all pointgroup elements leave $\mathbf{k} = (0,0)$ invariant, thus the little group of $\mathbf{k} = (0,0)$ is the full pointgroup. In general this does not hold for other momenta and only a subgroup of PG will be the little group of $\mathbf{k}$. In Fig. 4 we show the $\mathbf{k}$-points of a 6×6 triangular lattice together with its little groups as an example. The K point in the Brillouin zone has a D_3 little group, the M point a D_2 little group. Having discussed the representation theory for (symmorphic) space groups we state that the characters of these representations are just given by

$$\chi_{(\mathbf{k},\rho_{\mathbf{k}})}(\mathbf{t}, p) = \mathrm{e}^{i\mathbf{k}\cdot\mathbf{t}} \chi_{\rho_{\mathbf{k}}}(p) \tag{18}$$

where $\mathbf{t} \in \mathcal{T}$, $p \in \mathrm{PG}$ and $\chi_{\rho_{\mathbf{k}}}$ is the character of the representation $\rho_{\mathbf{k}}$ of the little group $L_{\mathbf{k}}$.

3.2 Predicting irreducible representations in spontaneous symmetry breaking

Spontaneous symmetry breaking at $T = 0$ occurs when the groundstate $|\psi_{\mathrm{GS}}\rangle$ of H in the thermodynamic limit is not invariant under the full symmetry group $\mathcal{G}$ of H. We will call a specific groundstate $|\psi_{\mathrm{GS}}\rangle$ a *prototypical state* and the *groundstate manifold* is defined by

$$V_{\mathrm{GS}} = \mathrm{span}\left\{|\psi_{\mathrm{GS}}^i\rangle\right\}, \tag{19}$$

where $|\psi_{\text{GS}}^i\rangle$ is the set of degenerate groundstates in the thermodynamic limit. This groundstate manifold space can be finite or infinite dimensional depending on the situation. For breaking a discrete finite symmetry, such as in the example given in section 4.1.2, this state will be finite dimensional, for breaking continuous $SO(3)$ spin rotational symmetry[6] as in section 4.2 this groundstate manifold is infinite dimensional in the thermodynamic limit. For every symmetry $g \in \mathcal{G}$ we denote by O_g the symmetry operator acting on the Hilbert space. The groundstate manifold becomes degenerate in the thermodynamic limit and we want to calculate the quantum numbers of the eigenstates in this manifold. Another way of saying this is that we want to compute the irreducible representations of $\mathcal{G}$ to which the eigenstates belong. For this we look at the action Γ of the symmetry group $\mathcal{G}$ on V_{GS} defined by

$$\Gamma : \mathcal{G} \to \text{Aut}(V_{\text{GS}}) \tag{20}$$

$$g \mapsto \left(\langle\psi_{\text{GS}}^i|O_g|\psi_{\text{GS}}^j\rangle\right)_{i,j} . \tag{21}$$

This is a representation of $\mathcal{G}$ on V_{GS}, so every group element $g \in \mathcal{G}$ is mapped to an invertible matrix on V_{GS}. In general this representation is reducible and can be decomposed into a direct sum of irreducible representations

$$\Gamma = \bigoplus_\rho n_\rho \rho . \tag{22}$$

These irreducible representations ρ are now the quantum numbers of the eigenstates in the groundstate manifold and n_ρ are their respective multiplicities (or degeneracies). Therefore these irreps constitute the TOS for spontaneous symmetry breaking [2]. To compute the multiplicities we can use a central result from representation theory, the *character formula*

$$n_\rho = \frac{1}{|\mathcal{G}|} \sum_{g \in \mathcal{G}} \overline{\chi_\rho(g)} \, \text{Tr}(\Gamma(g)) , \tag{23}$$

where $\chi_\rho(g)$ is the character of the representation ρ and $\text{Tr}(\Gamma(g))$ denotes the trace over the representation matrix $\Gamma(g)$ as defined in Eq. (20). Often we have the case that

$$\langle\psi_{\text{GS}}|O_g|\psi_{\text{GS}}'\rangle = \begin{cases} 1 & \text{if } O_g\,|\psi_{\text{GS}}'\rangle = |\psi_{\text{GS}}\rangle \\ 0 & \text{otherwise} \end{cases} \tag{24}$$

With this we can simplify Eq. (23) to what we call the *character-stabilizer formula*

$$n_\rho = \frac{1}{|\text{Stab}(|\psi_{\text{GS}}\rangle)|} \sum_{g \in \text{Stab}(|\psi_{\text{GS}}\rangle)} \chi_\rho(g) \tag{25}$$

where

$$\text{Stab}(|\psi_{\text{GS}}\rangle) \equiv \{g \in \mathcal{G} : \ O_g\,|\psi_{\text{GS}}\rangle = |\psi_{\text{GS}}\rangle\} \tag{26}$$

is the stabilizer of a prototypical state $|\psi_{\text{GS}}\rangle$. We see that for applying the character-stabilizer formula in Eq. (25) only two ingredients are needed:

---

[6]The actual symmetry group of Heisenberg antiferromagnets is usually $SU(2)$. For simplicity we only consider the subgroup $SO(3)$ in these notes which yields the same predictions for the case of sublattices with even number of sites (corresponding to integer total sublattice spin).

- the stabilizer $\text{Stab}(|\psi_{\text{GS}}\rangle)$ of a prototypical state $|\psi_{\text{GS}}\rangle$ in the groundstate manifold

- the characters of the irreducible representations of the symmetry group $\mathcal{G}$

We want to remark that in the case of $\mathcal{G} = \mathcal{D} \times \mathcal{C}$ where $\mathcal{D}$ is a discrete symmetry group, such as the spacegroup of a lattice, and $\mathcal{C}$ is a continuous symmetry group, such as $SO(3)$ rotations for Heisenberg spins, Eqs. (23) and (25) include integrals over Lie groups additionally to the sum over the elements of the discrete symmetry group $\mathcal{D}$. Furthermore, also the characters for Lie groups like $SO(3)$ are known. For an element $R \in SO(3)$ the irreducible representations are labeled by the spin S and its characters are given by

$$\chi_s(R) = \frac{\sin\left[(S + \frac{1}{2})\varphi\right]}{\sin(\varphi/2)}, \tag{27}$$

where $\varphi \in [0, 2\pi]$ is the angle of rotation of the spin rotation R. We work out several examples for this case in section 4.2 and compare the results to actual numerical data from Exact Diagonalization.

4 Examples

4.1 Discrete symmetry breaking

In this section we want to apply the formalism of section 3 to systems, where only a discrete symmetry group is spontaneously broken and not a continuous one. In this case, the ground-state of the system in the thermodynamic limit is described by a superposition of a finite number of degenerate eigenstates with different quantum numbers. On finite-size systems, however, the symmetry cannot be broken spontaneously and a unique groundstate will be found. The other states constituting the degenerate eigenspace in the thermodynamic limit exhibit a finite-size energy gap which is exponentially small in the system size N, $\Delta \propto \mathrm{e}^{-N/\xi}$. The quantum numbers of these quasi-degenerate sets of eigenstates are defined by the symmetry-broken state in the thermodynamic limit.

4.1.1 Introduction to valence-bond solids

In section 2 we have seen that the classically ordered Néel state is a candidate to describe the groundstate of the antiferromagnetic Heisenberg model Eq. (1) with $J > 0$ in the thermodynamic limit on a bipartite lattice. The energy expectation value of this state on each bond is $e_{\text{Néel}} = -J/4$.

The state which minimizes the energy of a single bond is, however, a singlet state $|S = 0\rangle$ formed by the two spins on the bond with energy $e_{\text{VB}} = -3J/4$, called a valence bond (VB) or dimer. A valence bond covering of an N-site lattice can then be described by a tensor product of $N/2$ VBs, where each site belongs to exactly one VB.[7] Another possible candidate for the

---

[7]The set of all possible valence bond coverings with arbitrary length spans the full $S_{\text{tot}} = 0$ sector of the models Hilbert space and is overcomplete [13, 14].
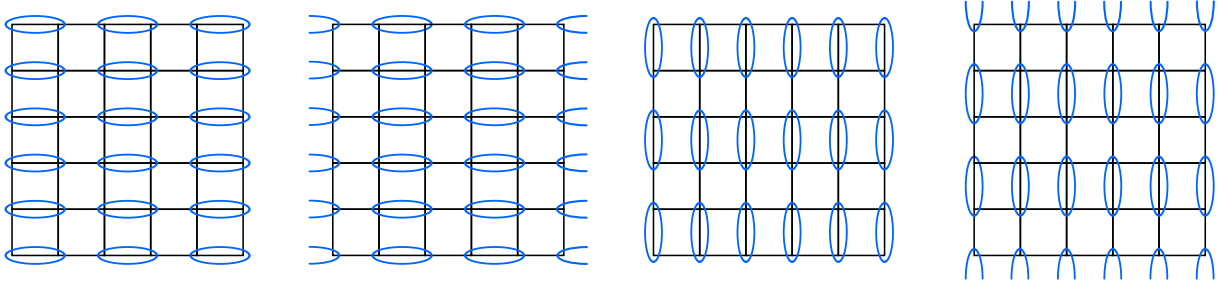
Fig. 2: *The four columnar VBS coverings of a square lattice. Valence bonds (spin singlets) are indicated by blue ellipses.*

thermodynamic groundstate of Eq. (1) is then a superposition of all possible VB coverings with nearest neighbor VBs. Such states do not break the $SU(2)$ spin-rotational symmetry as $S_{\text{tot}} = 0$ and are in general not eigenstates of the Hamiltonian: Acting with the operator $\mathbf{S}_i \cdot \mathbf{S}_j$ between sites i and j belonging to two different VBs changes the VB configuration.

This classical groundstate manifold is highly degenerate. As the VB coverings are in general not eigenstates of the Hamiltonian, they encounter quantum fluctuations. The energy corrections due to these fluctuations are usually not equivalent for different coverings, although the bare energies are identical. The VB coverings with the largest energy gain are selected by the fluctuations as the true groundstate configurations. If this *order-by-disorder* mechanism [15,16] selects regular patterns of VB coverings, the discrete lattice symmetries are spontaneously broken in the thermodynamic limit, and a *valence bond solid* (VBS) is formed. Fig. 2 and Fig. 3 show two different VBS states on the square lattice. VBSs show no long-range spin order, but long-range dimer-correlations $\langle (\mathbf{S}_a \cdot \mathbf{S}_{a'})(\mathbf{S}_b \cdot \mathbf{S}_{b'}) \rangle$ where a, a' and b, b' label sites on individual dimers. In section 4.1.2 we will see how different VBS states can be identified and distinguished by the quantum numbers of the quasi-degenerate groundstate manifold on finite-size systems.

The groundstate of the Heisenberg model Eq. (1) on the square lattice is not a VBS but a Néel state, which has already on the classical level a lower variational energy. Nevertheless, several models in 1- and 2-D are known which feature VBS groundstates [17–21]. Interestingly, in [22] a model was proposed, which shows a direct continuous quantum phase transition between a Néel state and a VBS. This transition exhibits very exotic, non-classical behavior and is called *deconfined quantum critical point* [23].

4.1.2 Identification of VBSs from finite-size spectra

Columnar valence-bond solid A columnar VBS (cVBS) on a square lattice is shown in Fig. 2. Four equivalent states can be found, indicating that there will be a four-fold quasi-degenerate groundstate manifold. A cVBS obviously breaks the translational and point-group symmetries of an isotropic $SU(2)$-invariant Hamiltonian on the lattice spontaneously but not the continuous spin symmetry group.

In the following we use Eq. (25) to compute the symmetry sectors of the groundstate manifold.

C_4	1	C_4	C_2	$(C_4)^3$
A	$+1$	$+1$	$+1$	$+1$
B	$+1$	-1	$+1$	-1
E_a	$+1$	$+i$	-1	$-i$
E_b	$+1$	$-i$	-1	$+i$

Table 1: *Character table for pointgroup* C_4.

The discrete symmetry group is

$$\mathcal{G} = \mathcal{D} = \mathcal{T} \times \mathrm{PG} \tag{28}$$

where $\mathcal{T} = \mathbb{Z}_2 \times \mathbb{Z}_2 = \{1, t_x, t_y, t_x t_y\}$ are the non-trivial lattice translations with translation vectors

$$\mathbf{t}_1 = (0,0), \quad \mathbf{t}_x = (1,0), \quad \mathbf{t}_y = (0,1), \quad \mathbf{t}_{xy} = (1,1) \tag{29}$$

and $\mathrm{PG} = C_4$ denotes the point-group of lattice rotations.[8] To compute the groundstate symmetry sectors we do not need to consider the full symmetry group $\mathcal{G}$ but only the stabilizer $\mathrm{Stab}(|\Psi_{cVBS}\rangle)$, leaving one of the states in Fig. 2 unchanged. Without loss of generality we choose the first covering as prototype $|\Psi_{cVBS}\rangle$. The stabilizer is given by

$$\mathrm{Stab}(|\Psi_{cVBS}\rangle) = \{1 \times 1\} \cup \{1 \times C_2\} \cup \{t_y \times 1\} \cup \{t_y \times C_2\} \tag{30}$$

where C_2 denotes the rotation about an angle π around the center of a plaquette.

The irreducible representations (irreps) of the group of lattice translations $\mathcal{T}$ can be labelled by the allowed momenta $\mathbf{k}$

$$\mathbf{k} \in \mathrm{Irreps}(\mathcal{T}) = \{(0,0), (\pi,0), (0,\pi), (\pi,\pi)\}, \tag{31}$$

and the corresponding characters for an element $t \in \mathcal{T}$ are

$$\chi_{\mathbf{k}}(t) = e^{i\mathbf{k} \cdot \mathbf{t}}. \tag{32}$$

The irreps (usually called A, B and E) and characters for the point-group C_4 are given in Tab. 1. Using Eq. (25) we can now reduce the representation induced by the state $|\Psi_{cVBS}\rangle$ to irreducible representations to get the quantum numbers of the quasi-degenerate groundstate manifold. Let us explicitly consider $n_{(\pi,0)A/B}$ as an example:

$$n_{(\pi,0)A} = \frac{1}{|\mathrm{Stab}(|\Psi_{cVBS}\rangle)|} \sum_{d \in \mathrm{Stab}(|\Psi_{cVBS}\rangle)} \chi_A(d)\, \chi_{\mathbf{k}=(\pi,0)}(d) \tag{33}$$

$$= \frac{1}{4} \left[1\, e^{i\mathbf{k} \cdot (0,0)} + 1\, e^{i\mathbf{k} \cdot (0,0)} + 1\, e^{i\mathbf{k} \cdot (0,1)} + 1\, e^{i\mathbf{k} \cdot (0,1)} \right] = 1 \tag{34}$$

$$n_{(\pi,0)B} = \frac{1}{|\mathrm{Stab}(|\Psi_{cVBS}\rangle)|} \sum_{d \in \mathrm{Stab}(|\Psi_{cVBS}\rangle)} \chi_B(d)\, \chi_{\mathbf{k}=(\pi,0)}(d) \tag{35}$$

$$= \frac{1}{4} \left[1\, e^{i\mathbf{k} \cdot (0,0)} + (-1)\, e^{i\mathbf{k} \cdot (0,0)} + 1\, e^{i\mathbf{k} \cdot (0,1)} + (-1)\, e^{i\mathbf{k} \cdot (0,1)} \right] = 0 \tag{36}$$

---

[8]The dihedral group D_4 is also a symmetry group of the model. For the sake of simplicity we decided to only consider the subgroup C_4 in this section.
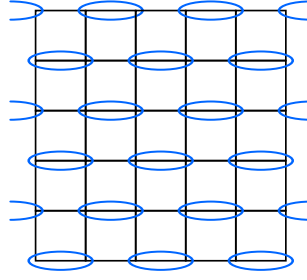
Fig. 3: *One of the four identical staggered VBS coverings on the square lattice.*

Eventually, the cVBS covering will be described by a four-fold quasi-degenerate groundstate manifold with the following quantum numbers

$$\chi(|\Psi_{cVBS}\rangle) = (0,0)A \oplus (0,0)B \oplus (\pi,0)A \oplus (0,\pi)A. \tag{37}$$

VBS states are a superposition of spin singlets on the lattice, therefore the spin quantum number for all levels in the groundstate manifold must be trivial, $S_{\text{tot}} = 0$.

Staggered valence-bond solid   The columnar VBS is not the only regular dimer covering of the square lattice. Another possible regular covering is the staggered VBS (sVBS), where again four equivalent configurations span the groundstate manifold. One of these configurations is shown in Fig. 3.

Obviously, also the sVBS spontaneously breaks the translational and point-group symmetries of an isotropic Hamiltonian, but not the spin-rotational symmetry. Following the same steps as before we can compute the quantum numbers of the four quasi-degenerate groundstates for the sVBS. The stabilizer turns out to be different to the case of the cVBS and thus also the decomposition into irreps yields a different result:

$$\chi(|\Psi_{sVBS}\rangle) = (0,0)A \oplus (0,0)B \oplus (\pi,\pi)E_a \oplus (\pi,\pi)E_b. \tag{38}$$

Tab. 2 shows a comparison of the irreducible representations in the groundstate manifold of the cVBS and sVBS states.

By a careful analysis of the quasi-degenerate states and their quantum numbers on finite systems it is thus possible to identify and distinguish different VBS phases which spontaneously break the translational and point-group symmetries in the thermodynamic limit.

Irreps	cVBS	sVBS
$(0,0)A$	1	1
$(0,0)B$	1	1
$(\pi,0)A$	1	0
$(0,\pi)A$	1	0
$(\pi,\pi)E_a$	0	1
$(\pi,\pi)E_b$	0	1

Table 2: *Multiplicities of the irreducible representations in the four-fold degenerate groundstate manifolds of the columnar and staggered VBS on a square lattice.*

4.2 Continuous symmetry breaking

In this section we give several examples of systems breaking continuous $SO(3)$ symmetry. We discuss the introductory example of the Heisenberg antiferromagnet, calculate the irreps in the TOS and compare this to actual energy spectra from Exact Diagonalization on a finite lattice in section 4.2.1. Next we discuss three magnetic orders on the triangular lattice and a model where all of these are stabilized. We show again results from Exact Diagonalizations and compare the representations in these spectra to the predictions from TOS analysis in section 4.2.2. Finally we introduce quadrupolar order and show that also this kind of symmetry breaking can be analyzed using the TOS technique in section 4.2.3.

4.2.1 Heisenberg antiferromagnet on square lattice

We now give a first example how the TOS method can be applied to predict the structure of the tower of states for magnetically ordered phases. We look at the Néel state of the antiferromagnet on the bipartite square lattice with sublattices A and B. A prototypical state in the groundstate manifold is given by

$$|\psi\rangle = |\uparrow\downarrow\uparrow\downarrow\cdots\rangle \tag{39}$$

where all spins point up on sublattice A and down on sublattice B. The symmetry group $\mathcal{G} = \mathcal{D} \times \mathcal{C}$ of the model we consider is a product between discrete translational symmetry $\mathcal{D} = \mathbb{Z}_2 \times \mathbb{Z}_2 = \{1, t_x, t_y, t_{xy}\}$ and spin rotational symmetry $\mathcal{C} = SO(3)$. We remark that we restrict our translational symmetry group to $\mathcal{D} = \mathbb{Z}_2 \times \mathbb{Z}_2$ instead of $\mathcal{D}' = \mathbb{Z} \times \mathbb{Z}$ because the Néel state transforms trivially under two-site translations $(t_x)^2, (t_y)^2$. Thus, only the representations of $\mathcal{D}'$ trivial under two-site translations are relevant; these are exactly the representations of $\mathcal{D}$. Put differently we only have to consider the translations in the unitcell of the magnetic structure which in the present case can be chosen as a 2-by-2 cell. Furthermore, we will for now neglect pointgroup symmetries like rotations and reflections of the lattice to simplify our calculations. At the end of this section we give results where also these symmetry elements are incorporated. The groundstate manifold V_{GS} we consider are the states related to $|\psi\rangle$ by an element of the symmetry group $\mathcal{G}$, i.e.,

$$V_{\text{GS}} = \{O_g |\psi\rangle \,;\; g \in \mathcal{G}\} \,. \tag{40}$$

The symmetry elements in $\mathcal{G}$ that leave our prototypical state $|\psi\rangle$ invariant are given by two sets of elements:

- No translation in real space or a diagonal t_{xy} translation together with a spin rotation $R_z(\alpha)$ around the z-axis with an arbitrary angle α.

- Translation by one site, t_x or t_y, followed by a rotation $R_a(\pi)$ of 180° around an axis $a \perp z$ perpendicular to the z-axis.

So the stabilizer of our prototype state $|\psi\rangle$ is given by

$$\text{Stab}(|\psi\rangle) = \{1 \times R_z(\alpha)\} \cup \{t_{xy} \times R_z(\alpha)\} \cup \{t_x \times R_a(\pi)\} \cup \{t_y \times R_a(\pi)\} \,. \tag{41}$$

The representations of the discrete symmetry group can be simply labeled by four momenta $\mathbf{k} \in \{(0,0),\ (0,\pi),\ (\pi,0),\ (\pi,\pi)\}$ with corresponding characters

$$\chi_{\mathbf{k}}(t) = e^{i\mathbf{k}\cdot\mathbf{t}}.$$

The continuous symmetry group is the Lie group $SO(3)$. Its representations are labeled by the total spin S and the character of the spin-S representation is given by

$$\chi_S(R) = \frac{\sin\left[(S+\frac{1}{2})\varphi\right]}{\sin(\varphi/2)}$$

where $\varphi \in [0, 2\pi]$ is the angle of rotation of the element $R \in SO(3)$. We see that spin rotations with different axes but same rotational angle give rise to the same character. The representations of the total symmetry group $\mathcal{G} = \mathcal{D} \times \mathcal{C}$ are now just the product representations of $\mathcal{D}$ and $\mathcal{C}$, therefore also the characters of representations of $\mathcal{G}$ are the product of characters of $\mathcal{D}$ and $\mathcal{C}$. We label these representations by $(\mathbf{k}, S)$ where $\mathbf{k}$ denotes the lattice momentum and S the total spin. We now apply the character-stabilizer formula, Eq. (25), to derive the multiplicities of the representations $(\mathbf{k}, S)$ in the groundstate manifold. In the case of the square antiferromagnet this yields

$$n_{(\mathbf{k},S)} = e^{i\mathbf{k}\cdot 0}\frac{1}{4\left|R_z(\alpha)\right|}\int\limits_0^{2\pi} d\alpha\, \chi_S(R_z(\alpha)) + e^{i\mathbf{k}\cdot(\mathbf{e}_x+\mathbf{e}_y)}\frac{1}{4\left|R_z(\alpha)\right|}\int\limits_0^{2\pi} d\alpha\, \chi_S(R_z(\alpha)) \tag{42}$$

$$+ e^{i\mathbf{k}\cdot\mathbf{e}_x}\frac{1}{4\left|R_a(\pi)\right|}\int\limits_0^{2\pi} d\alpha\, \chi_S(R_a(\pi)) + e^{i\mathbf{k}\cdot\mathbf{e}_y}\frac{1}{4\left|R_a(\pi)\right|}\int\limits_0^{2\pi} d\alpha\, \chi_S(R_a(\pi))\,. \tag{43}$$

We compute

$$\left|R_z(\alpha)\right| = \left|R_a(\pi)\right| = \int\limits_0^{2\pi} d\varphi = 2\pi\,,$$

$$\frac{1}{2\pi}\int\limits_0^{2\pi} d\alpha\, \chi_S(R_z(\alpha)) = \frac{1}{2\pi}\int\limits_0^{2\pi} d\alpha\, \frac{\sin\left[(S+\frac{1}{2})\alpha\right]}{\sin(\alpha/2)} = \frac{1}{2\pi}\int\limits_0^{2\pi} d\varphi \sum_{l=-S}^{S} e^{il\varphi} = 1\,, \tag{44}$$

and

$$\frac{1}{2\pi}\int\limits_0^{2\pi} d\varphi\, \chi_S(R_a(\pi)) = \frac{1}{2\pi}\int\limits_0^{2\pi} d\varphi\, \frac{\sin\left[(S+\frac{1}{2})\pi\right]}{\sin(\pi/2)} = (-1)^S. \tag{45}$$

Putting this together gives the final result for the multiplicities of the representations in the tower

S	$\Gamma.A1$	$M.A1$
0	1	0
1	0	1
2	1	0
3	0	1

Table 3: *Multiplicities of irreducible representations in the TOS for the Néel antiferromagnet on a square lattice.*

of states

$$n_{((0,0),S)} = \frac{1}{4}\left(1\cdot 1 + 1\cdot 1 + 1\cdot(-1)^S + 1\cdot(-1)^S\right) = \begin{cases} 1 \text{ if } S \text{ even} \\ 0 \text{ if } S \text{ odd} \end{cases} \tag{46}$$

$$n_{((\pi,\pi),S)} = \frac{1}{4}\left(1\cdot 1 + 1\cdot 1 - 1\cdot(-1)^S - 1\cdot(-1)^S\right) = \begin{cases} 0 \text{ if } S \text{ even} \\ 1 \text{ if } S \text{ odd} \end{cases} \tag{47}$$

$$n_{((0,\pi),S)} = \frac{1}{4}\left(1\cdot 1 - 1\cdot 1 + 1\cdot(-1)^S - 1\cdot(-1)^S\right) = 0 \tag{48}$$

$$n_{((\pi,0),S)} = \frac{1}{4}\left(1\cdot 1 - 1\cdot 1 - 1\cdot(-1)^S + 1\cdot(-1)^S\right) = 0 \tag{49}$$

Tab. 3 lists the computed multiplicities of the irreducible representations where additionally the D_4 point group was considered in the symmetry analysis. Comparing this to Fig. 1 we observe that these are exactly the irreducible representations (momenta and point group irreps) and multiplicities observed in the tower of states for the Heisenberg model on the square lattice.

4.2.2 Magnetic order on the triangular lattice

On the triangular lattice several magnetic orders can be stabilized. The Heisenberg nearest neighbor model has been shown to have a 120° Néel ordered groundstate where spins on neighboring sites align in an angle of 120° [24, 25]. Upon adding further second nearest neighbor interactions J_2 to the Heisenberg nearest-neighbor model with interaction strength J_1 it was shown that the groundstate exhibits *stripy order* for $J_2/J_1 \gtrsim 0.18$ [26]. Here spins are aligned ferromagnetically along one direction of the triangular lattice and antiferromagnetically along the other two. Interestingly, it was shown that there is a phase between these two magnetic orders whose exact nature is unclear until today. Several articles propose that in this region an exotic *quantum spin liquid* is stabilized [27–30]. In a recent proposal two of the authors established an approximate phase diagram of an extended Heisenberg model with further scalar chirality interactions $J_\chi \mathbf{S}_i \cdot (\mathbf{S}_j \times \mathbf{S}_k)$ [31] on elementary triangles. Thus, the Hamiltonian of the system is given by

$$\mathcal{H} = J_1 \sum_{\langle i,j \rangle} \mathbf{S}_i \cdot \mathbf{S}_j + J_2 \sum_{\langle\langle i,j \rangle\rangle} \mathbf{S}_i \cdot \mathbf{S}_j + J_\chi \sum_{i,j,k \in \triangle} \mathbf{S}_i \cdot (\mathbf{S}_j \times \mathbf{S}_k). \tag{50}$$

Amongst the already known 120° Néel and stripy phases an exotic *Chiral Spin Liquid* and a magnetic *tetrahedrally ordered* phase were found. Here we will only discuss the magnetic
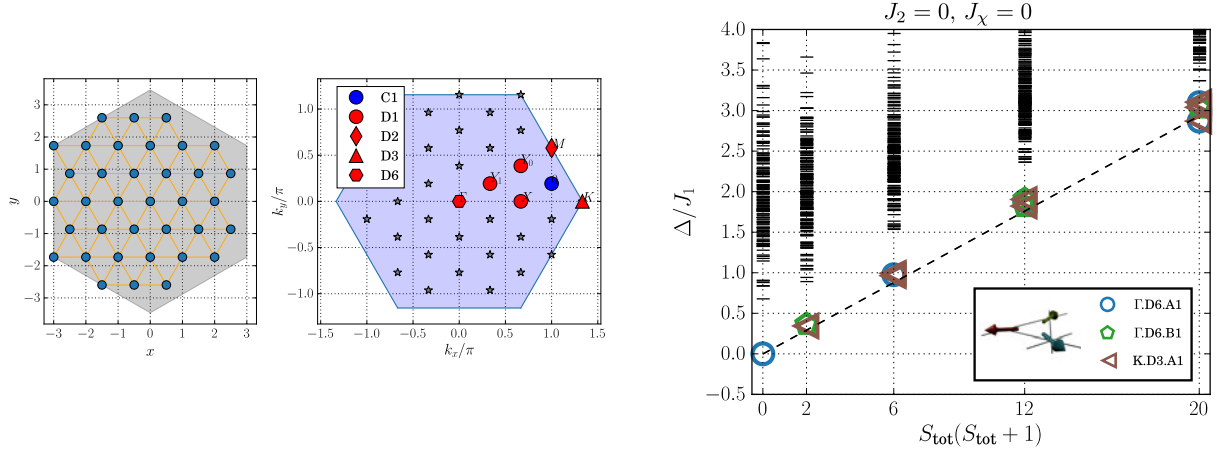
Fig. 4: *(Left): Simulation cluster for the Exact Diagonalization calculations. (Center): Brillouin zone of the triangular lattice with the momenta which can be resolved with this choice of the simulation cluster. Different symbols denote the little groups of the corresponding momentum. (Right): TOS for the $120°$ Néel order on the triangular lattice. The symmetry sectors and multiplicities fulfill the predictions from the symmetry analysis (See Tab. 5). One should note, that the multiplicities grow with S_{tot} for non-collinear states.*

orders appearing in this model. The non-coplanar tetrahedral order has a four-site unitcell where four spins align such that they span a regular tetrahedron. In this chapter we show the tower of states for the three magnetic orders in this model.

First of all, Fig. 4 shows the simulation cluster used for the Exact Diagonalization calculations in [31]. We chose a $N = 36 = 6 \times 6$ sample with periodic boundary conditions. This sample allows to resolve the momenta Γ, K and M, amongst several others in the Brillouin zone. The K and M momenta are the ordering vectors for the $120°$, stripy and tetrahedral order. Furthermore this sample features full six-fold rotational as well as reflection symmetries (the latter only in the absence of the chiral term). Its pointgroup is therefore given by the dihedral group of order 12, D_6. The little groups of the individual $\mathbf{k}$ vectors are also shown in Fig. 4. For our tower of states analysis we now want to consider the discrete symmetry group

$$\mathcal{D} = \mathcal{T} \times \mathrm{D}_6 \tag{51}$$

where $\mathcal{T}$ is the translational group of the magnetic unitcell. The full set of irreducible representations of this symmetry group is given by the set $(\mathbf{k} \otimes \rho_{\mathbf{k}})$ where $\mathbf{k}$ denotes the momentum and $\rho_{\mathbf{k}}$ is an irrep of the little group associated to $\mathbf{k}$. The points Γ, K and M give rise to the little groups D_6, D_3 and D_2 (the dihedral groups of order 12, 8, and 4), respectively. For the stripy and tetrahedral order we can choose a 2×2 magnetic unitcell, and a 3×3 unitcell for the $120°$ Néel order. The spin rotational symmetry lets us again consider the continuous symmetry group

$$\mathcal{C} = SO(3). \tag{52}$$

We can therefore label the full set of irreps as $(\mathbf{k}, \rho_{\mathbf{k}}, S)$ where S denotes the total spin S representation of $SO(3)$. Similarly to the previous chapter we now want to apply the character-stabilizer formula, Eq. (25), to determine the multiplicities of the representations forming the

D_6	1	$2C_6$	$2C_3$	C_2	$3\sigma_d$	$3\sigma_v$
A_1	1	1	1	1	1	1
A_2	1	1	1	1	-1	-1
B_1	1	-1	1	-1	1	-1
B_2	1	-1	1	-1	-1	1
E_1	2	1	-1	-2	0	0
E_2	2	-1	-1	2	0	0

Table 4: *Character table for pointgroup D_6.*

	120° Néel			stripy order			tetrahedral order			
S	Γ.A1	Γ.B1	K.A1	Γ.A1	Γ.E2	M.A	Γ.A	Γ.E2a	Γ.E2b	M.A
0	1	0	0	1	1	0	1	0	0	0
1	0	1	1	0	0	1	0	0	0	1
2	1	0	2	1	1	0	0	1	1	1
3	1	2	2	0	0	1	1	0	0	2

Table 5: *Multiplicities of irreducible representations in the Anderson tower of states for the three magnetic orders on the triangular lattice defined in the main text.*

tower of states. The characters of the irreps $(\mathbf{k}, \rho_{\mathbf{k}}, S)$ are given by

$$\chi_{(\mathbf{k},\rho_{\mathbf{k}},S)}(t, p, R) = e^{i\mathbf{k}\cdot\mathbf{t}}\chi_{\rho_{\mathbf{k}}}(p)\frac{\sin\left[(S + \frac{1}{2})\varphi\right]}{\sin(\varphi/2)}, \tag{53}$$

where again $\varphi \in [0, 2\pi]$ is the angle of rotation of the spin rotation R. The characters of the pointgroup D_6 are given in Tab. 4. We skip the exact calculations which follow closely the calculations performed in the previous chapter, although now also pointgroup symmetries are additionally taken into account. The results are summarized in Tab. 5. We remark that the tetrahedral order is stabilized only for $J_\chi \neq 0$ where the model in Eq. (50) does not have reflection symmetry any more since the term $\mathbf{S}_i \cdot (\mathbf{S}_j \times \mathbf{S}_k)$ does not preserve this symmetry. Therefore we used only the pointgroup C_6 of six-fold rotation in the calculations of the tower of states for this order.

If we compare these results to Figs. 4 and 5 we see that these are exactly the representations appearing in the TOS from Exact Diagonalization for certain parameter values J_2 and J_χ. This is a strong evidence that indeed $SO(3)$ symmetry is broken in these models in a way described by the 120° Néel, stripy, and tetrahedral magnetic prototype states.

4.2.3 Quadrupolar order

All examples of continuous symmetry breaking we have discussed so far spontaneously broke $SO(3)$ symmetry but exhibited a magnetic moment. In the following we will show examples of phases that do not exhibit any magnetic moment but break spin-rotational symmetry anyway and discuss the influences on the tower of states. We will only discuss quadrupolar phases in $S = 1$ models here, a broader introduction to nematic and multipolar phases can be found in [32].
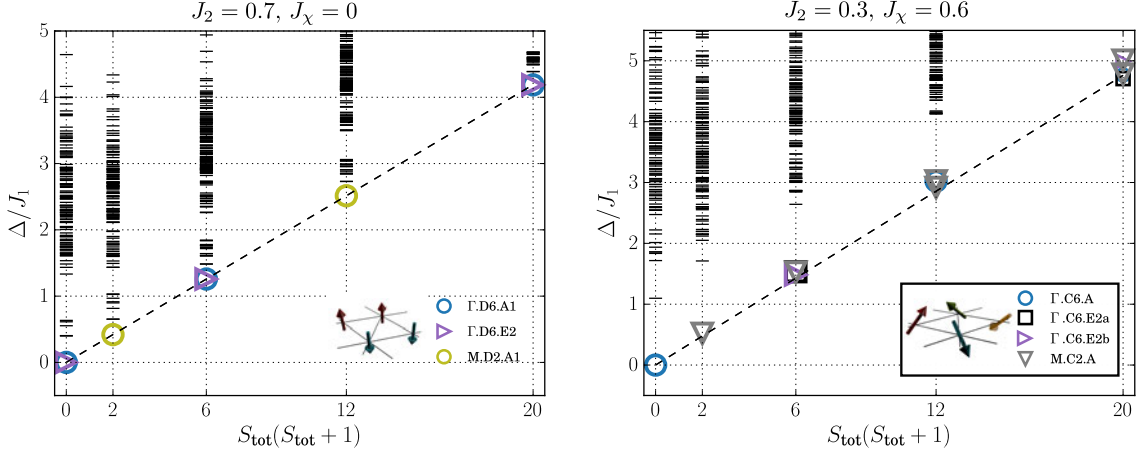
Fig. 5: *(Left): TOS for the stripy phase on the triangular lattice. The multiplicities for each even/odd S_{tot} are constant for collinear phases. (Right): TOS for the tetrahedral order on the triangular lattice.*

Quadrupolar states We denote the basis states for a single spin $S = 1$ with $S^z = 1, -1, 0$ as $|1\rangle, |\bar{1}\rangle, |0\rangle$. In contrast to the usual $S = 1/2$ case not each basis state can be obtained by a SU(2) rotation of any other basis state. The state $|0\rangle$, for example cannot be obtained by a rotation of $|1\rangle$ or $|\bar{1}\rangle$ as it has no orientation in spin-space at all, $\langle 0|S^\alpha|0\rangle = 0$ [32]. The state $|0\rangle$ can, however, be described as a spin fluctuating in the x-y plane in spin space as

$$\langle 0|(S^x)^2|0\rangle = \langle 0|(S^y)^2|0\rangle = 1, \quad \langle 0|(S^z)^2|0\rangle = 0. \tag{54}$$

We can thus assign a director along the z-axis to this state. $SU(2)$ rotations will change the director of such a state, but not its property of being non-magnetic. These states can be detected by utilizing the quadrupolar operator [32]

$$Q^{\alpha\beta} = S^\alpha S^\beta + S^\beta S^\alpha - \frac{2}{3}S(S+1)\delta_{\alpha\beta} \tag{55}$$

therefore they are identified as quadrupolar states.

To study the possible formation of an ordered quadrupolar phase on a lattice, where the directors of the quadrupoles on each lattice site follow a regular pattern, we consider the *bilinear-biquadratic* model with Hamiltonian

$$H = \sum_{\langle i,j\rangle} J\, \mathbf{S}_i \cdot \mathbf{S}_j + Q\left(\mathbf{S}_i \cdot \mathbf{S}_j\right)^2 \tag{56}$$

and $S = 1$. The second term in Eq. (56) can be rewritten in terms of the elements of $Q^{\alpha\beta}$ which can be rearranged into a 5-component vector $\mathbf{Q}$ such that

$$\mathbf{Q}_i \cdot \mathbf{Q}_j = 2(\mathbf{S}_i \cdot \mathbf{S}_j)^2 + \mathbf{S}_i \cdot \mathbf{S}_j - \frac{4}{3}. \tag{57}$$

The expectation value of Eq. (57) for quadrupolar states on sites i and j can be given in terms of their directors $\mathbf{d}_{i,j}$ [32]

$$\langle \mathbf{Q}_i \cdot \mathbf{Q}_j\rangle = 2\left(\mathbf{d}_i \cdot \mathbf{d}_j\right)^2 - \frac{2}{3}. \tag{58}$$

Therefore, the second term in Eq. (56) favors regular patterns of the directors of quadrupoles. When such states are formed, they spontaneously break the $SU(2)$ symmetry without exhibiting any kind of magnetic moment. The first term in Eq. (56), on the other hand, favors spin ordering as we have already discussed in previous sections.

The phase diagram of Eq. (56) on the triangular lattice shows extended ferromagnetic, antiferromagnetic ($120°$), ferroquadrupolar (FQ), and antiferroquadrupolar (AFQ) ordered phases. In the FQ phase quadrupoles on each lattice site are formed with all directors pointing in a single direction, whereas the directors form a $120°$ structure in the AFQ phase. In the following, we will see that the FQ and AFQ phases can be identified and distinguished from the spin ordered phases using a tower-of-states analysis on finite clusters.

TOS for quadrupolar phases   The TOS for the FQ and AFQ phases can be expected to show similar behavior as the TOS for magnetically ordered states as both spontaneously break the spin-rotational symmetry. If we identify the symmetry-broken quadrupolar phases with their directors pointing in any direction in spin-space we can perform the symmetry analysis of the TOS levels in a very similar manner as for the spin-ordered systems in the previous sections. There is, however, one important thing to consider: The directors should not be considered to be described with vectors, but with axes; a quadrupole is recovered (up to a phase) by rotations about an angle π around any axis a in the x-y-plane:

$$\mathrm{e}^{i\pi S^a} |0\rangle = - |0\rangle \,. \tag{59}$$

Thus, the stabilizer in Eq. (25) is different for quadrupolar phases and the TOS shows a different structure. This property makes it possible to distinguish, e.g., a magnetic $120°$ phase from its quadrupolar counterpart, the AFQ phase, with a TOS analysis.

A prototype for the FQ phase is a product states of quadrupoles with directors in z-direction, $|\Psi\rangle = |0, 0, 0, \ldots\rangle$. This state does not break any space-group symmetries, so only the trivial irreps of the space group, $\mathbf{k} = \Gamma = (0,0).A1$, will be present in the TOS. The remaining stabilizer of the spin-rotation group is a rotation about the z-axis by an arbitrary angle and a rotation about an arbitrary axis lying in the x-y-plane,

$$\mathrm{Stab}(|\Psi\rangle) = \{R_z(\alpha), R_a(\pi)\}. \tag{60}$$

The multiplicities in the TOS can then be computed as

$$n_S = \frac{1}{2} \left(\frac{1}{|R_z(\alpha)|} \int_0^{2\pi} d\alpha \, \chi_S(R_z(\alpha)) + (-1)^N \frac{1}{|R_a(\pi)|} \int_0^{2\pi} da \, \chi_S(R_a(\pi)) \right) \tag{61}$$

$$= \frac{1}{2} \left(1 + (-1)^N (-1)^S \right), \tag{62}$$

where the integrals have already been computed in Eqs. (44) and (45). The system size dependent factor $(-1)^N$ is imposed from Eq. (59). To sum up, the TOS for the FQ phase has single levels for even (odd) S with trivial space-group irreps and no levels for odd (even) S
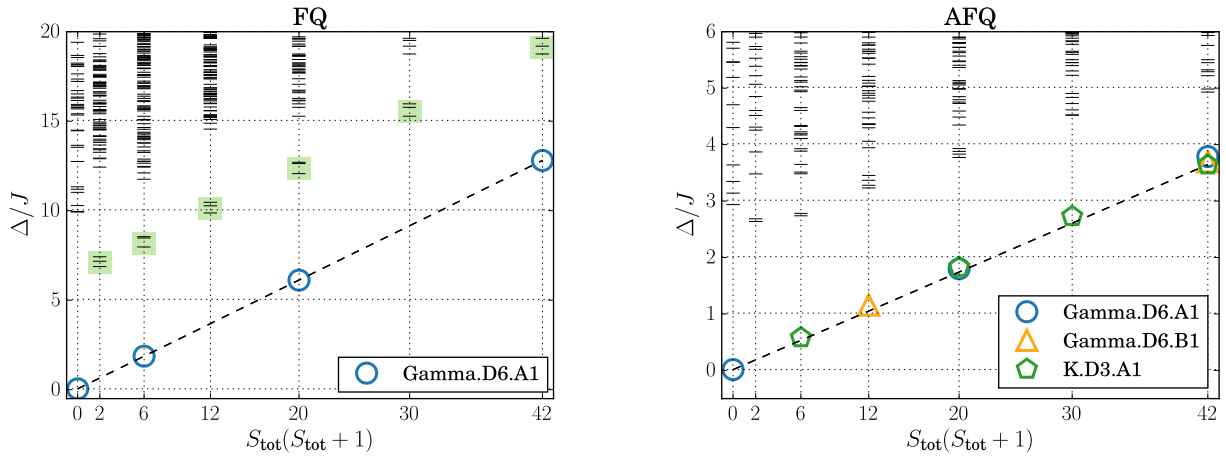
Fig. 6: *Tower of states for the ferroquadrupolar (left) and antiferroquadrupolar (right) states on a triangular lattice with $N = 12$ sites from Exact Diagonalization. The single-magnon branch for the FQ phase is highlighted with green boxes.*

sectors when N is even (odd).[9] The absence of odd (even) S levels is caused by the invariance of quadrupoles under π-rotation and distinguishes the TOS for a FQ phase from a usual ferromagnetic phase. In Fig. 6 the TOS for the model, Eq. (56), in the FQ phase is shown on the left. It shows the expected quantum numbers and multiplicities in the TOS and also an easily identifiable magnon branch below the continuum.

The symmetry analysis for the AFQ phase can be performed in a similar manner and shows a similar structure to the 120°-Néel phase, but again, levels are deleted for the AFQ. In this case, however, not all odd levels are deleted but some levels in both, odd and even, S sectors. Tab. 6 shows the multiplicities of irreps in the TOS of the AFQ model in comparison to the magnetic 120°-Néel state for even N. Fig. 6 shows the simulated TOS for the AFQ phase for the bilinear-biquadratic model Eq. (56). The symmetry sectors and multiplicities agree with the expected ones.

S	AFQ Γ.A1	Γ.B1	K.A1	120° Néel Γ.A1	Γ.B1	K.A1
0	1	0	0	1	0	0
1	0	0	0	0	1	1
2	0	0	1	1	0	2
3	0	1	0	1	2	2

Table 6: *Irreducible representations and multiplicities for the AFQ phase compared to the magnetic 120°-Néel phase.*

---

[9] For the simple case of the FQ phase one can also easily calculate the decomposition of a state $|S = 1, m = 0\rangle \otimes |S = 1, m = 0\rangle \otimes \ldots$ into states $|S_{tot}, m = 0\rangle$ with the use of Clebsch-Gordan coefficients.

5   Outlook

In the previous sections we have discussed the features of the energy spectrum for states which spontaneously break the spin-rotational symmetry, $SU(2)$, in the thermodynamic limit. We have seen that on finite-size systems the energy spectra of such states exhibit a tower of states (TOS) structure. The tower of states scales as $S_{\text{tot}}(S_{\text{tot}} + 1)/N$ and generates the groundstate manifold in the thermodynamic limit $N \to \infty$, which is indispensable to spontaneously break a symmetry. The quantum numbers of the levels in the TOS depend on the particular state which is formed after the symmetry breaking and can be predicted using representation theory.

As a generalization to the $SU(2)$-symmetric Heisenberg model, Eq. (1), one can introduce $SU(n)$ Heisenberg models with $n > 2$. Such models can experimentally be realized by ultra-cold multicomponent fermions in a optical lattices. When the on-site repulsion is strong enough, the Hamiltonian can be effectively described by an $SU(n)$-symmetric permutation model on the lattice [33]. When the exchange couplings are antiferromagnetic, $SU(n)$ generalized versions of the Néel state might be realized as groundstates, which then spontaneously break the $SU(n)$ symmetry of the Hamiltonian. On finite systems this becomes again manifest in the emergence of a tower of states, where the scaling is found to be proportional to $C_2(n)/N$ [34–37, 33]. $C_2(n)$ denotes the quadratic Casimir operator of $SU(n)$.[10] The symmetry analysis of the levels in the TOS can, in principle, be performed similar to the case of $SO(3)$ discussed in these notes, but the symmetry group and its characters have to be replaced with the more complicated group $SU(n)$.

On the other side, it can be also interesting to study models where the continuous symmetry group is smaller. In real magnetic materials, the isotropic Heisenberg interaction is often accompanied by other interactions which, when they are strong enough, might reduce the symmetry group of spin rotations from $SO(3)$ to $O(2)$; only spin rotations around an axis are a symmetry of the system and can be spontaneously broken in the thermodynamic limit. This symmetry group is also interesting in the field of ultracold gases, as BECs spontaneously break an $O(2)$ symmetry by choosing a phase. Tower of states can also be found in this case and the quantum numbers and multiplicities of the TOS levels can be computed similar to the $SU(2)$ case [12].

We have seen, that the energy spectrum of Hamiltonians on finite lattices may contain a lot of information about the system. One can identify groundstates which will spontaneously break discrete as well as continuous symmetries in the thermodynamic limit and by imposing a classical state as symmetry-broken state one can even predict the quantum numbers and multiplicities of the levels in the tower of states or in the quasi-degenerate groundstate manifold. When we impose an additional interaction to a system with spontaneously broken groundstate, e.g., a magnetic field, it is possible that a *continuous quantum phase transition* (cQPT) from the ordered state to a disordered state appears for some critical ratio of the couplings. Such cQPTs are interesting as they can be described by universal features which do not depend on the details of

---

[10]For $n = 2$ the quadratic Casimir operator $C_2 = S_{\text{tot}}(S_{\text{tot}} + 1)$.
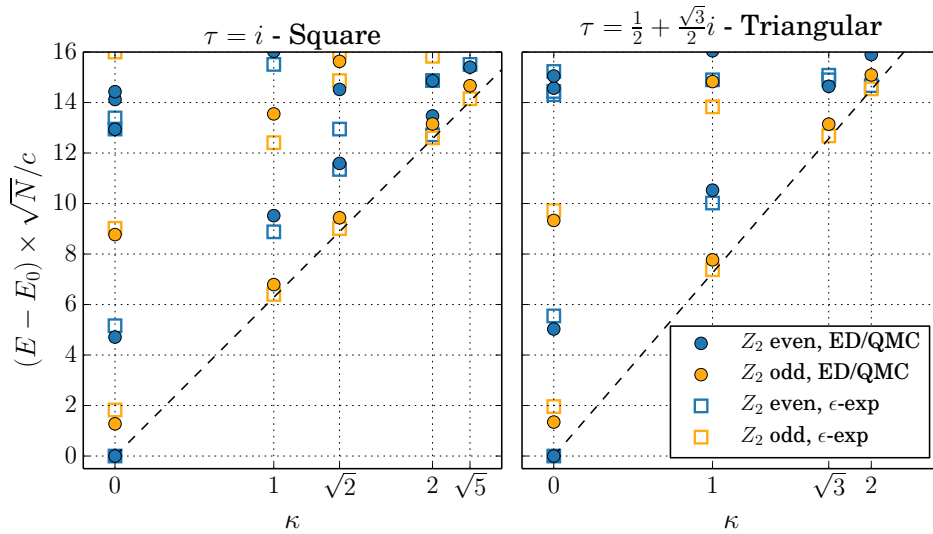
Fig. 7: *Universal torus spectrum for a continuous quantum phase transition in the 3D Ising universality class. Full symbols denote numerical results while empty symbols denote ϵ-expansion results. The dashed line shows a dispersion with the speed of light.*

the model. Interestingly, the energy spectrum on finite systems can even be used to identify and characterize cQPTs. It is given by universal numbers times $1/L$, where $L = \sqrt{N}$ is the linear size of the lattice. The quantum numbers of the energy levels show universal features and are related to the operator content of the underlying *critical field theory*, although the relation between them is not yet fully understand for non-flat geometries, like a torus [38, 39]. The critical spectrum for the transverse-field Ising model on a torus is shown in Fig. 7. It is a fingerprint for the 3D Ising cQPT.

References

[1] P.W. Anderson, Phys. Rev. **86**, 694 (1952)

[2] C. Lhuillier, arXiv:cond-mat pp. 161–190 (2005)

[3] A.M. Läuchli: *Numerical Simulations of Frustrated Systems*
(Springer, Heidelberg, 2011), pp. 481–511

[4] A.W. Sandvik, A. Avella, and F. Mancini:
in *AIP Conf. Proc.* (2010), Vol. 1297, pp. 135–338

[5] G. Misguich and P. Sindzingre, J. Phys. Condens. Matter **19**, 145202 (2007)

[6] W. Marshall, Proc. R. Soc. A Math. Phys. Eng. Sci. **232**, 48 (1955)

[7] E. Lieb and D. Mattis, Journal of Mathematical Physics **3**, 749 (1962)

[8] A. Auerbach: *Interacting Electrons and Quantum Magnetism* (Springer, New York, 1994)

[9] T.A. Kaplan, W. von der Linden, and P. Horsch, Phys. Rev. B **42**, 4663 (1990)

[10] P. Hasenfratz and F. Niedermayer, Zeitschrift für Phys. B Condens. Matter **92**, 91 (1993)

[11] P. Azaria, B. Delamotte, and D. Mouhanna, Phys. Rev. Lett. **70**, 2483 (1993)

[12] I. Rousochatzakis, A.M. Läuchli, and F. Mila, Phys. Rev. B **77**, 094420 (2008)

[13] S. Liang, B. Doucot, and P.W. Anderson, Phys. Rev. Lett. **61**, 365 (1988)

[14] C. Lhuillier and G. Misguich: In C. Lacroix, P. Mendels, and F. Mila (Eds.): *Introduction to Frustrated Magnetism*, *Springer Series in Solid-State Sciences*, Vol. 164
(Springer, Heidelberg, 2011), pp. 23–41

[15] E. Shender, Sov. Phys. JETP **56**, 178 (1982)

[16] C.L. Henley, Phys. Rev. Lett. **62**, 2056 (1989)

[17] J. Fouet, P. Sindzingre, and C. Lhuillier, Eur. Phys. J. B **20**, 241 (2001)

[18] A. Läuchli, S. Wessel, and M. Sigrist, Phys. Rev. B **66**, 014401 (2002)

[19] A. Läuchli, J.C. Domenge, C. Lhuillier, P. Sindzingre, and M. Troyer,
Phys. Rev. Lett. **95**, 137206 (2005)

[20] M. Mambrini, A. Läuchli, D. Poilblanc, and F. Mila, Phys. Rev. B **74**, 144422 (2006)

[21] A. Gellé, A.M. Läuchli, B. Kumar, and F. Mila, Phys. Rev. B **77**, 014419 (2008)

[22] A.W. Sandvik, Phys. Rev. Lett. **98**, 227202 (2007)

[23] T. Senthil, A. Vishwanath, L. Balents, S. Sachdev, and M.P.A. Fisher,
     Science **303**, 1490 (2004)

[24] T. Jolicoeur, E. Dagotto, E. Gagliano, and S. Bacci, Phys. Rev. B **42**, 4800 (1990)

[25] A. V. Chubukov and T. Jolicoeur, Phys. Rev. B **46**, 11137 (1992)

[26] P. Lecheminant, B. Bernu, C. Lhuillier, and L. Pierre, Phys. Rev. B **52**, 6647 (1995)

[27] Y. Iqbal, W.-J. Hu, R. Thomale, D. Poilblanc, and F. Becca,
     Phys. Rev. B **93**, 144411 (2016)

[28] R. Kaneko, S. Morita, and M. Imada, J. Phys. Soc. Jpn. **83**, 093707 (2014)

[29] W.-J. Hu, S.-S. Gong, W. Zhu, and D.N. Sheng, Phys. Rev. B **92**, 140403 (2015)

[30] Z. Zhu and S.R. White, Phys. Rev. B **92**, 041105 (2015)

[31] A. Wietek and A.M. Läuchli, ArXiv e-prints (2016)

[32] K. Penc and A.M. Läuchli: *Spin Nematic Phases in Quantum Spin Systems*
     (Springer Berlin, Heidelberg, 2011), pp. 331–362

[33] P. Nataf and F. Mila, Phys. Rev. Lett. **113**, 127204 (2014)

[34] K. Penc, M. Mambrini, P. Fazekas, and F. Mila, Phys. Rev. B **68**, 012408 (2003)

[35] T. A. Tóth, A.M. Läuchli, F. Mila, and K. Penc, Phys. Rev. Lett. **105**, 265301 (2010)

[36] P. Corboz, A.M. Läuchli, K. Penc, M. Troyer, and F. Mila,
     Phys. Rev. Lett. **107**, 215301 (2011)

[37] P. Corboz, M. Lajkó, K. Penc, F. Mila, and A.M. Läuchli, Phys. Rev. B **87**, 195113 (2013)

[38] M. Schuler, S. Whitsitt, L.-P. Henry, S. Sachdev, and A.M. Läuchli, arXiv:1603.03042

[39] S. Whitsitt and S. Sachdev, arXiv:1603.05652